282 OPTICS LETTERS / Vol. 13, No. 4 / April 1988

Tunable holographic second-harmonic generators in high-birefringence optical fibers

M. E. Fermann, M. C. Farries, P. St. J. Russell, and L. Poyntz-Wright

Optical Fibre Group, Department of Electronics and Computer Science, University of Southampton, Southampton S09 5NH, UK

Received November 24, 1987; accepted January 22, 1988

The formation of efficient holographic second-harmonic generators in high-birefringence phosphorus-doped germanosilicate fibers is reported. The influence of optical polarization on the nonlinear writing and read-out processes is explored. Fiber birefringence permits phase-matched second-harmonic conversion at wavelengths within $\pm 125\ cm^{-1}$ (± 14 nm) of the writing wavelength (1.064 μm).

There is now reasonable agreement in the literature over the underlying cause of anomalous growth in second-harmonic generation (SHG) observed[1] in lightly phosphorus-doped germanosilicate fibers subjected to sustained exposure at 1.064 μm. The basic mechanism[2,3] is the electric-field polarization provided by a $\chi^{(3)}$ optical rectification process involving two pump photons and a second-harmonic (SH) photon. The resulting periodically reversing internal dc field gives rise to the alignment of as yet unidentified non-inversion-symmetric defect centers and hence to a periodically modulated $\chi^{(2)}$. This $\chi^{(2)}$ grating provides the phase matching needed for high conversion efficiencies in an apparently amorphous medium. Recently the effect was seen at 647.1 nm in pure germanosilicate fibers.[4]

Stolen and Tom[3] showed that a $\chi^{(2)}$ grating may be created within minutes if a pair of mutually coherent pump and second-harmonic waves are launched simultaneously into the fiber in a process reminiscent of holography. The resulting nonlinear $\chi^{(2)}$ hologram can then be used to generate the SH from a reference beam at the pump wavelength, with conversion efficiencies (depending on the phosphorus dopant levels) of the order of 1%.

We examine here the influence of fiber birefringence on this phenomenon both for its intrinsic interest and in order to clarify the nature of the induced $\chi^{(2)}$ nonlinearity. To facilitate the measurements we fabricated a high-birefringence (HiBi) germanosilicate bow-tie fiber with a numerical aperture of 0.24 and a phosphorus content of approximately 2% as estimated from the deposition conditions. The fiber core (see Fig. 1) was elliptical with an aspect ratio of 3 and was drawn to be single mode at 1064 nm and to support the E_{11}, E_{21}, and E_{12} modes at 532 nm. Its birefringence $B(\lambda)$ was measured as 4.8×10^{-4} at 1064 nm and estimated to be about 2.2×10^{-4} for the E_{11} mode at 532 nm. Its birefringence dispersion $\partial B/\partial\lambda$ in the vicinity of these two wavelengths was measured to be $1.38 \times 10^{-3}\ \mu m^{-1}$ at 1064 nm and effectively zero at 532 nm. Over the 1-m fiber length used in our experiments, cross coupling between the two polarization states amounted to approximately 1% of the total output power.

To interpret our results, we needed an approximate expression for the dispersion of the effective mode indices in the fiber. We used Sellmeier expansions for the material dispersion of the P-doped germanosilicate core[5] and the P_2O_5–F-doped cladding. These were combined with the expression derived by Gloge[6] for the effective index $N(\lambda)$ of the E_{11} mode in a circular fiber (equivalent core radius taken to be 1 μm). When the measured birefringence was distributed equally on either side of $N(\lambda)$, the effective fast (f) and slow (s) fiber indices could then be approximated:

$$N_{s(f)}(\lambda) = N(\lambda) \pm 0.5[B(\lambda_0) + (\lambda - \lambda_0)\partial B(\lambda_0)/\partial\lambda], \quad (1)$$

where λ_0 is chosen according to whether the effective indices in the vicinity of 532 or 1064 nm are required.

Given that light polarized along both the fast and the slow axes can be present during the seeding stage, the internal dc field takes the form

$$\mathbf{E}_0^{(3)}[0] = (1/3)\chi^{(3)}_{1111}\{(\mathbf{E}_0[\omega_0]\cdot\mathbf{E}_0[\omega_0])\mathbf{E}_0^*[2\omega_0] + 2\mathbf{E}_0[\omega_0](\mathbf{E}_0[\omega_0]\cdot\mathbf{E}_0^*[2\omega_0]) + \text{c.c.}\}, \quad (2)$$

where the electric fields are

$$\mathbf{E}_0[\omega] = \sum_{k=f,s} kA_{k0}[\omega]\exp\{j\omega[t - N_k(\omega)x/c]\} \quad (3)$$

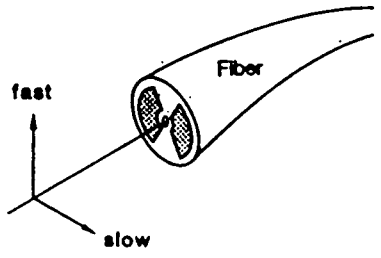

Fig. 1. Schematic view of the bow-tie HiBi fiber (outer diameter 125 μm) fabricated for the experiments. The P-doped core was elliptical, with major and minor dimensions across the core of approximately 3 and 1 μm.

0146-9592/88/040282-03$2.00/0

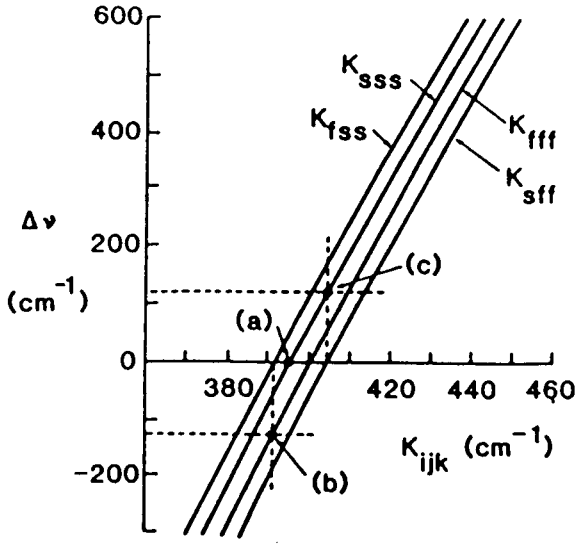

Fig. 2. The dispersion of the grating vectors K_{ijk} (expressed as $K_{ijk}/2\pi$ in inverse centimeters) relevant to the three cases treated in the experiments. Phase matching is achieved in case (b) at $\Delta\nu = -123$ cm^{-1} from 1064 nm and in case (c) at $\Delta\nu = +121$ cm^{-1}.

and the normal symmetry relations for $\chi^{(3)}$ in a dispersion-free isotropic medium are assumed, i.e., $\chi^{(3)}_{1221} = \chi^{(3)}_{1212} = \chi^{(3)}_{1122} = \frac{1}{3}\chi^{(3)}_{1111}$. The subscripts 0 denote the seeding process, and the refractive indices N_k follow Eq. (1). A_{f0} and A_{s0} equal half of the actual fast and slow electric field amplitudes, x is the axial fiber coordinate, c is the velocity of light *in vacuo*, and ω its angular frequency. The unit vectors $\hat{f}$ and $\hat{s}$ are parallel to the fast and slow axes. The assumption[3] is that $\chi^{(2)}$ aligns parallel to $E_0^{(3)}[0]$, resulting in general in the formation of several different $\chi^{(2)}$ holograms whose grating vectors are given by

$$K_{ijk}(\omega_0) = \{2\omega_0/c\}\{N_i[2\omega_0] - 0.5(N_j[\omega_0] + N_k[\omega_0])\}, \quad (4)$$

where i, j, and k can equal s or f.

We shall now restrict the discussion to three simple cases in which the fundamental and SH seed polarizations are aligned exactly along the HiBi axes of the fiber. From Eq. (2) an immediate consequence of this restriction is that $\chi^{(2)}$ will always be oriented parallel to the SH polarization for cases of perfect f or s alignment of the seed polarizations. We consider the three cases

(a) $A_{s0}(2\omega_0)$ and $A_{s0}(\omega_0)$ nonzero, grating vector $K_{sss}(\omega_0)$;
(b) $A_{f0}(2\omega_0)$ and $A_{s0}(\omega_0)$ nonzero, grating vector $K_{fss}(\omega_0)$;
(c) $A_{s0}(2\omega_0)$ and $A_{f0}(\omega_0)$ nonzero, grating vector $K_{sff}(\omega_0)$.

Phase matching will occur at any pump frequency ω for which the fixed grating vector precisely equals the wave-vector mismatch between two pump and one SH wave vector, i.e., when

$$\text{(a)}\quad K_{sss}(\omega_0) = K_{sss}(\omega),$$
$$\text{(b)}\quad K_{fss}(\omega_0) = K_{fff}(\omega),$$
$$\text{(c)}\quad K_{sff}(\omega_0) = K_{sss}(\omega). \quad (5)$$

For example, in case (b) phase-matched conversion occurs between a fast pump and a fast SH at a frequency (see Fig. 2) less than ω_0.

To test these predictions, $\chi^{(2)}$ holograms were produced by launching Q-switched mode-locked pulses of 2-kW peak power from a Nd:YAG laser into the fiber. A $LiIO_3$ crystal was inserted at the output of the laser to provide a mixture of about 4% SH at 532 nm and 96% pump at 1064 nm, where both waves were linearly polarized and orthogonal to each other. A half-wave plate (at 1064 nm) was used to change the relative polarization orientations of the writing pump and the SH. Dispersion in the plate introduced a maximum 10% ellipticity into the writing SH when its polariza-

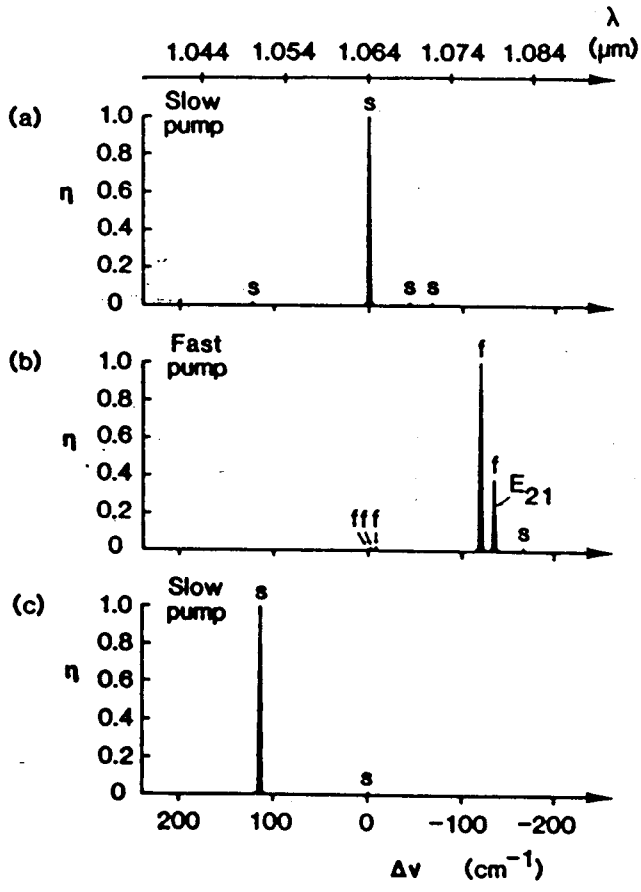

Fig. 3. The measured SH conversion η as a function of wavenumber deviation $\Delta\nu$ from the writing pump wavelength, 1064 nm, for the three cases in Fig. 2. In this figure (and in Fig. 4) η is normalized to its maximum measured value in each case. Notice that phase-matched conversion to the SH E_{12} mode occurs at 135 cm^{-1} in case (b). The presence of slow- or fast-polarized SH light is denoted by the letter s or f, respectively. The peaks marked fs are mixed (see text). The additional minor conversion peaks are caused by inevitable small misalignments of the polarization during writing and read-out and poor polarization-preserving properties in the fiber used.

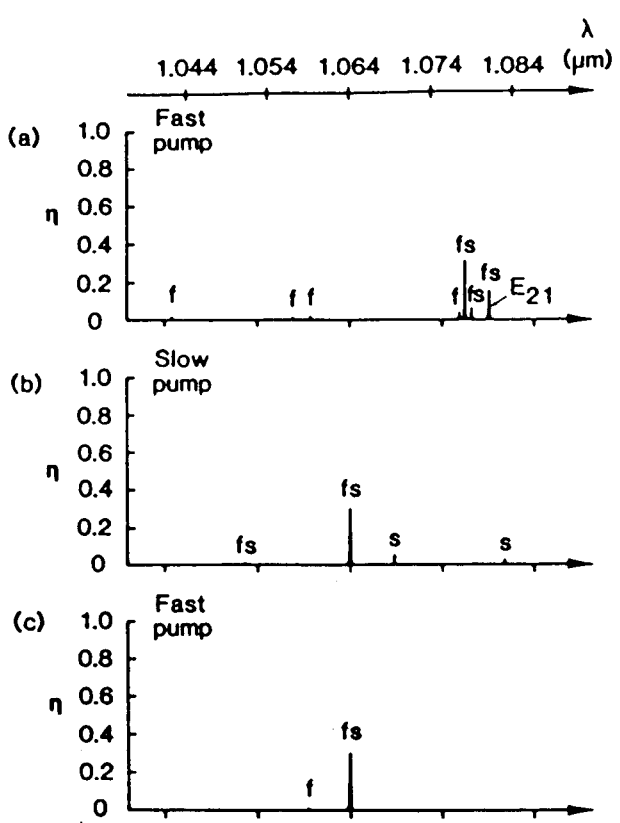

Fig. 4. As in Fig. 3, except that the read-out pump polarization is orthogonal to the expected alignment direction of $\chi^{(2)}$. The conversion efficiencies η are normalized to the maximum measured values in Fig. 3. For perfect alignment of the writing and reading polarization the conversion efficiencies here would be zero.

tion was aligned at 45° to the plate's major axis. SH conversion efficiencies of ~1% were obtained at pump powers of 400 W after 15 min of writing. Competing nonlinear effects (stimulated Brillouin and Raman scattering, self-phase modulation) meant that the conversion efficiency saturated at about 1% for powers in excess of 400 W. The wavelength and polarization dependence of the SH conversion efficiency was then probed with a Raman-shifted dye laser delivering pulses of 6-nsec duration over a tuning range 1030–1090 nm. The probe-pulse peak power was ~10 W, and the polarization of the probe pulses was adjusted with a compensator.

The measured conversion efficiency as a function of frequency deviation $\Delta\nu$ from 1064 nm is shown in Fig. 3 for the three cases mentioned above. The SH was generated predominantly in the E_{11} mode. Conversion to the SH E_{21} mode, which occurs through inevitable minor radial asymmetries in the input coupling of the SH writing light, was observed only in case (b). Numerical solutions of Eqs. (5) for conversion to the SH E_{11} mode predict conversion peaks at 1.078 μm (case b) and 1.051 μm (case c), which agree almost exactly with the measurement. Our simple theory does not predict the minor peaks visible in Fig. 3. They may, however, be explained by recourse to a more detailed approach in which inaccuracies in alignment, the relatively poor polarization-preserving properties of the fiber (1% cross-coupled intensity represents 10% in dc field terms), and axial nonuniformities in birefringence are taken into account. These alignment inaccuracies lead also to substantial conversion efficiencies when the orthogonal read-out pump polarization state is chosen (see Fig. 4). The elliptically polarized conversion peaks suggest that phase matching is achieved simultaneously at the same wavelength for both fast and slow SH signals. This odd result is an artifact of our inability to resolve several closely spaced peaks, some of which are slow and others fast polarized. Our tentative conclusion, from careful measurements, is that no unusual off-axis terms (apart from a possible $\chi_{zyy}^{(2)}$, $\chi_{zzz}^{(2)}$ being the principal on-diagonal term and y the other transverse fiber axis) exist in the induced second-order susceptibility. This agrees with the lack of any alignment mechanism normal to the dc field, something that would be essential for the creation of a macroscopic $\chi_{yzy}^{(2)}$.

In summary, fiber birefringence can be used to generate phase-matched SH at wavelengths other than the writing wavelength, 1064 nm. In view of the maximum birefringence achievable in HiBi fibers, efficient SH generators functioning at frequencies within 125 cm^{-1} (±14 nm) of 1064 nm are possible. This is of special interest for frequency-doubling fiber lasers.[7] A simple model for the writing process, allowing for different polarization states of the writing pump and the SH, leads to the result that the generated $\chi^{(2)}$ nonlinearity aligns with the SH. This is corroborated in the experimental measurements. When both material and waveguide dispersion are taken into account, good agreement is achieved between the observed and calculated wavelengths of highest SH conversion efficiency.

References

1. U. Österberg and W. Margulis, Opt. Lett. 12, 57 (1987).
2. M. C. Farries, P. St. J. Russell, M. E. Fermann, and D. N. Payne, Electron. Lett. 23, 322 (1987).
3. R. H. Stolen and H. W. K. Tom, Opt. Lett. 12, 585 (1987).
4. B. Valk, E. M. Kim, and M. M. Salour, Appl. Phys. Lett. 51, 722 (1987).
5. J. W. Fleming, Electron. Lett. 14, 326 (1978).
6. D. Gloge, Appl. Opt. 10, 2252 (1971).
7. L. Reekie, R. J. Mears, S. B. Poole, and D. N. Payne, IEEE J. Lightwave Technol. LT-4, 956 (1986).